



ERNEST ORLANDO LAWRENCE BERKELEY NATIONAL LABORATORY

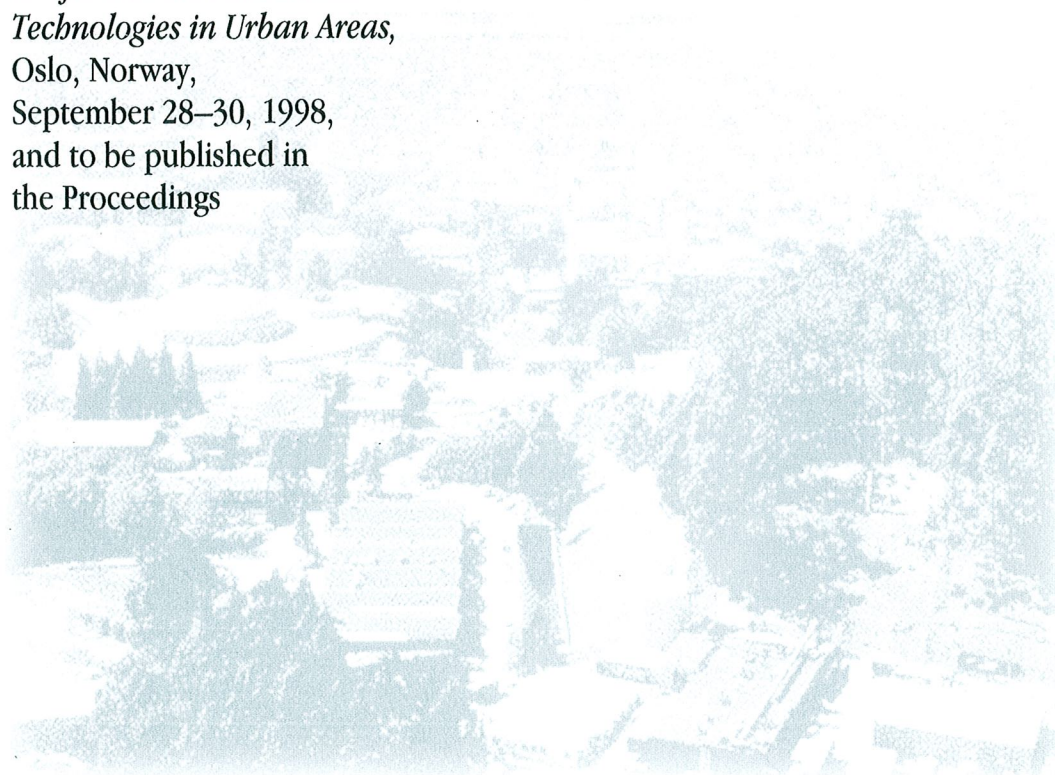
CFD Simulation of Infiltration Heat Recovery

C.R. Buchanan and M.H. Sherman

**Environmental Energy
Technologies Division**

July 1998

Invited paper to be
presented at the
*19th AIVC Annual
Conference on Ventilation
Technologies in Urban Areas,*
Oslo, Norway,
September 28–30, 1998,
and to be published in
the Proceedings



DISCLAIMER

This document was prepared as an account of work sponsored by the United States Government. While this document is believed to contain correct information, neither the United States Government nor any agency thereof, nor The Regents of the University of California, nor any of their employees, makes any warranty, express or implied, or assumes any legal responsibility for the accuracy, completeness, or usefulness of any information, apparatus, product, or process disclosed, or represents that its use would not infringe privately owned rights. Reference herein to any specific commercial product, process, or service by its trade name, trademark, manufacturer, or otherwise, does not necessarily constitute or imply its endorsement, recommendation, or favoring by the United States Government or any agency thereof, or The Regents of the University of California. The views and opinions of authors expressed herein do not necessarily state or reflect those of the United States Government or any agency thereof, or The Regents of the University of California.

Ernest Orlando Lawrence Berkeley National Laboratory
is an equal opportunity employer.

CFD Simulation of Infiltration Heat Recovery

C.R. Buchanan and M.H. Sherman

Environmental Energy Technologies Division
Indoor Environment Department
Energy Performance of Buildings Group
Lawrence Berkeley National Laboratory
University of California
Berkeley, CA

July 1998

This work was supported by the Assistant Secretary for Energy Efficiency and Renewable Energy, Office of Building Technology of the U.S. Department of Energy under Contract No. DE-AC03-76SF00098.

CFD Simulation of Infiltration Heat Recovery

C. R. Buchanan and M. H. Sherman¹

Energy Performance of Buildings Group
Indoor Environment Department
Environmental Energy Technologies Division
Lawrence Berkeley National Laboratory
University of California

Abstract

Infiltration has traditionally been assumed to affect the energy load of a building by an amount equal to the product of the infiltration flow rate and the sensible enthalpy difference between inside and outside. Results from detailed computational fluid dynamics simulations of five wall geometries over a range of infiltration rates show that heat transfer between the infiltrating air and walls can be substantial, reducing the impact of infiltration. Factors affecting the heat recovery are leakage path length, infiltration flow rate, and wall construction. The classical method for determination of the infiltration energy load was found to over-predict the amount by as much as 95 percent and by at least 10 percent. However, the air flow paths typical of building envelopes give over-predictions at the low end of this range.

Nomenclature

c_p = specific heat capacity of air (1006 J/kg K)
 c_{ps} = specific heat capacity of insulation solid component (1006 J/kg K)
 c_{pw} = specific heat capacity of wall sheathing (1200 J/kg K)
 g = gravity (9.81 m/s²)
 k = air thermal conductivity (0.025 W/m K)
 k_{eff} = effective thermal conductivity of insulation (0.025 W/m K)
 k_s = thermal conductivity of insulation solid component (0.041 W/m K)
 k_w = wall sheathing thermal conductivity (0.13 W/m K)
 Q = total (conduction and convection) heat load (W)
 Q_{inf} = energy load due to infiltration (W)
 Q_{infC} = classical energy load due to infiltration (W)
 Q_o = pure conduction heat load (W)
 m = infiltration mass flow rate (kg/s)
 p = air pressure (Pa)
 t = time (s)
 T = temperature (K)
 T_i = inside air temperature (298 K)

¹ LBNL-42098: This work was supported by the Assistant Secretary for Energy Efficiency and Renewable Energy, Office of Building Technology of the U.S. Department of Energy under contract no. DE-AC03-76SF00098.

T_o = outside air temperature (274 K)
 T_s = temperature of insulation solid component (K)
 T_w = wall sheathing temperature (K)
 u = air flow velocity in x-direction (m/s)
 v = air flow velocity in y-direction (m/s)
 x = horizontal co-ordinate (m)
 y = vertical co-ordinate (m)

α = insulation permeability (10^{-8} m^2)
 $\Delta T = T_i - T_o$ (24 K)
 ε = infiltration heat exchange effectiveness or heat recovery factor (dim)
 ϕ = mass fraction of air in wall insulation material (0.99)
 μ = air viscosity ($1.72 \times 10^{-5} \text{ kg/m s}$)
 ρ = air density (kg/m^3)
 ρ_s = density of insulation solid component (70 kg/m^3)
 ρ_w = wall sheathing density (544 kg/m^3)

Introduction

Air leakage through building envelopes, infiltration, is a common phenomenon, which affects both indoor air quality and building energy consumption. Some researchers have studied the potential of reducing building energy consumption by intentionally incorporating this process into the building design (3,9,15). In this technique, known as dynamic insulation, air is drawn through the building envelope in a direction that opposes the natural conductive flow of energy, so that some portion of the energy ordinarily lost to conduction is recovered.

In the most buildings, however, infiltration is unintentional and uncontrolled. Claridge and Bhattacharyya (7) note that a great deal of work has been devoted to the prediction and measurement of infiltration in building systems, but little effort has been directed toward determining the actual energy impact of infiltration. Infiltration can contribute a significant amount to the overall heating or cooling load of a building, but the actual size of the effect depends on a host of factors, including environmental conditions, building design, and construction quality. Based on experimental measurements taken at 50 residential buildings, Caffey (5) concluded that up to 40 percent of the heating/cooling costs in the homes studied was due to infiltration. In another study of residential buildings, Persily (13) attributed about one-third of the heating/cooling requirements to infiltration. Sherman and Matson (14) examined measured leakage data and concluded that a high fraction of the space conditioning load in U.S. buildings was due to infiltration. The results of a recent study (12) of U.S. office buildings performed by the National Institute of Standards and Technology (NIST) show that air leakage accounts for about 15 percent of the heating load in office buildings nationwide and about 1 or 2 percent of the cooling load. By all measures, the impact of infiltration can be sizeable and, so, should be considered in calculations of building energy consumption.

$$Q_{\text{infC}} = \dot{m}c_p(T_i - T_o) \quad (1)$$

The traditional method of accounting for the extra load due to infiltration is to simply add another term to the energy balance, denoted here as the classical infiltration load. The extra term, shown in equation 1, is the product of the infiltrating air mass flow rate, the specific heat capacity of air, and the temperature difference between inside and outside. This relation does not include the effects of moisture in the air and is strictly valid only if the leaking air does not interact thermally with the building walls. In reality, leaking air exchanges heat with the walls as it enters and leaves the building, which changes the thermal profile in the walls and warms or cools the infiltrating/exfiltrating air. This results in different values for the conduction, infiltration, and total heat losses than are predicted by the traditional method. Some studies have shown that this effect could be quite substantial and that the traditional method incorrectly predicts the energy impact of infiltration (2,6,7,10).

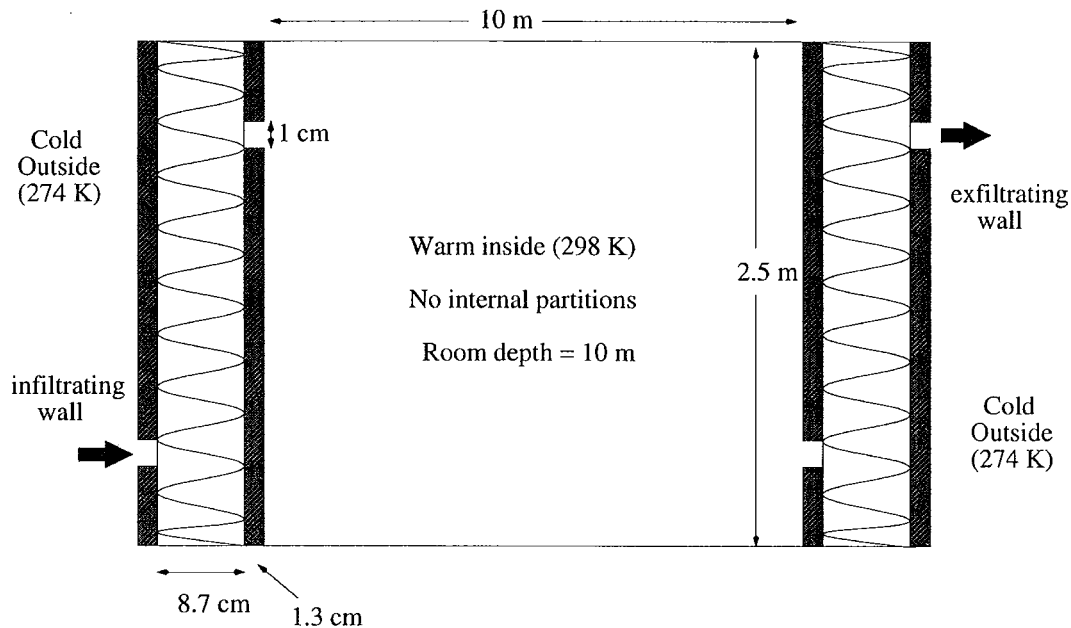


Figure 1: General problem setup; wall geometry 1 shown.

The purpose of this paper is to investigate the potential heat transfer between infiltrating air and room walls, known as heat recovery, and how this process could affect the additional energy requirements due to infiltration. Previous studies have measured lump values experimentally (2,6,7) or simulated the system using simplified modeling, for example, a prescribed Nusselt number for the air-wall heat transfer (10). This study determines the individual contributions of conduction and convection to the total heating load via numerical simulation without making simplifications regarding the basic physical processes involved. A commercial computational fluid dynamics (CFD) package is used to simulate the air flow and heat transfer through a two-dimensional wall section.

The general problem setup is shown in figure 1. Small holes, or cracks, in the outer sheathing (plywood) allow air to leak into the wall cavity and flow through the wall from outside to inside and vice-versa. Five wall configurations, shown in figure 2, are examined under various environmental conditions. Wall geometries 1-3 have insulation in the wall cavity, while geometries 4 and 5 have empty wall cavities. Geometries 1 and 4 provide a long flow path for infiltrating air that could potentially create a displacement flow in the wall cavity. Geometries 2 and 5 provide a short flow path for infiltrating air that could likely isolate air in the top and bottom sections of the wall. Geometry 3 has the possibility for both long and short paths. Pressure differences across the walls are varied from 0.1-10 Pa and the

inside/outside temperature difference remains constant at 24 Kelvin. The pressure differentials are taken to represent wind-induced pressures caused by wind flowing around the building, but they could also be induced by mechanical ventilation systems.

An advantage of CFD simulations over experimental studies is that many important aspects of the problem which are often difficult to determine, like boundary conditions, material properties, and flow paths, are known exactly and can be systematically varied easily. This makes correlations between different variables, for example, air flow path length and heat recovery, much more reliable. A disadvantage of such simulations is that it is difficult to represent the complexity of the true system, especially the variations associated with construction quality and material properties. The systems here are idealized, having homogeneous material properties and perfect construction, and will give conservative results. Though, these results should be representative and of practical value with proper interpretation.

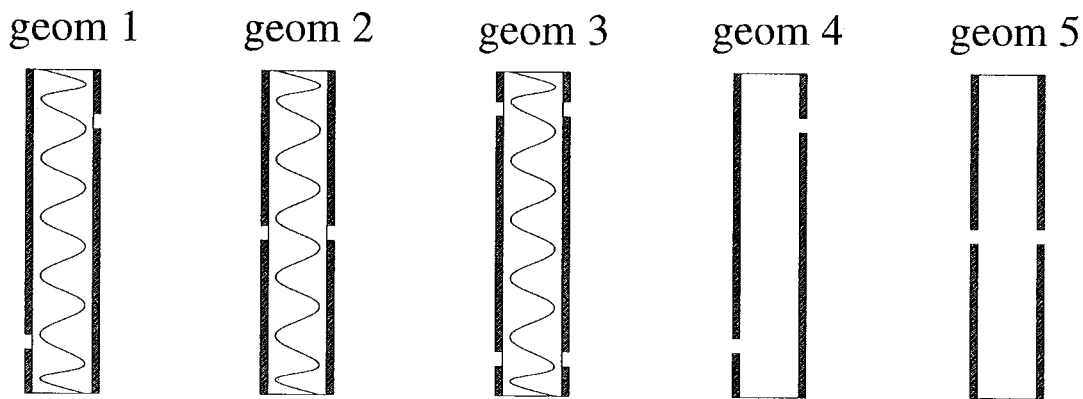


Figure 2: The five wall geometries examined; 1,2, & 3 are insulated and 4 & 5 are empty.

Problem Formulation

The example room in this study represents a row-house inner unit (figure 1) and is composed of an infiltrating wall, a corresponding exfiltrating wall, and a ceiling, floor, front wall, and rear wall with no air leakage. The building envelope is separated into non-interacting wall elements, which are examined individually. Information from the individual walls is added together to determine the overall impact for a complete room system. The windward and leeward walls, both of the same geometry type, are matched by their air leakage rates and have crack lengths that extend the entire depth of the wall (10 m). The bulk air flow within the room is not represented, but this should not be a problem because, as Etheridge (8) notes, the internal room air flow has only a secondary effect on infiltration. The most important influences are wind-induced pressure differences and buoyancy of room air in the vicinity of the wall.

The wall section is modeled as a two-dimensional, time-dependent system. Air flow and energy transport within the air are determined via the Navier-Stokes and energy equations (equations 2-5), respectively. A laminar representation is used for the flow, and solutions show this to be a valid assumption, as the highest predicted Reynolds number is only about 2000. Velocities elsewhere in the flow are much lower and would not provide the

potential for turbulence. The plywood sheathing is represented as an impermeable, solid material. Energy transport within the sheathing is calculated via the conduction equation (equation 6). Insulation in the wall is represented as a porous material. Air flow through the insulation is determined via Darcy's Law (equations 7 & 8), a common model for flow through porous media (4,10). Energy transport through the insulation is determined via a modified form of the energy equation (equation 9). In equation 9, an effective conductivity, given by equation 10, is used in the conduction flux term and the thermal inertia of the solid component is included in the transient term.

$$\frac{\partial \rho}{\partial t} + \frac{\partial \rho u}{\partial x} + \frac{\partial \rho v}{\partial y} = 0 \quad (2)$$

$$\frac{\partial \rho u}{\partial t} + \frac{\partial \rho u u}{\partial x} + \frac{\partial \rho u v}{\partial y} = -\frac{\partial p}{\partial x} + \mu \frac{\partial}{\partial x} \left[2 \frac{\partial u}{\partial x} - \frac{2}{3} \left(\frac{\partial u}{\partial x} + \frac{\partial v}{\partial y} \right) \right] + \mu \frac{\partial}{\partial y} \left(\frac{\partial u}{\partial y} + \frac{\partial v}{\partial x} \right) \quad (3)$$

$$\frac{\partial \rho v}{\partial t} + \frac{\partial \rho u v}{\partial x} + \frac{\partial \rho v v}{\partial y} = -\frac{\partial p}{\partial y} + \rho g + \mu \frac{\partial}{\partial x} \left(\frac{\partial u}{\partial y} + \frac{\partial v}{\partial x} \right) + \mu \frac{\partial}{\partial y} \left[2 \frac{\partial v}{\partial y} - \frac{2}{3} \left(\frac{\partial u}{\partial x} + \frac{\partial v}{\partial y} \right) \right] \quad (4)$$

$$c_p \frac{\partial \rho T}{\partial t} + c_p \frac{\partial \rho u T}{\partial x} + c_p \frac{\partial \rho v T}{\partial y} = k \frac{\partial^2 T}{\partial x^2} + k \frac{\partial^2 T}{\partial y^2} + \frac{\partial p}{\partial t} + u \frac{\partial p}{\partial x} + v \frac{\partial p}{\partial y} \quad (5)$$

$$\rho_w c_{pw} \frac{\partial T_w}{\partial t} = k_w \frac{\partial^2 T_w}{\partial x^2} + k_w \frac{\partial^2 T_w}{\partial y^2} \quad (6)$$

$$\frac{\partial p}{\partial x} = -\frac{\mu}{\alpha} u \quad (7) \quad , \quad \frac{\partial p}{\partial y} = -\frac{\mu}{\alpha} v \quad (8)$$

$$\frac{\partial}{\partial t} (\phi c_p \rho T + (1-\phi) c_{ps} \rho_s T_s) + c_p \frac{\partial \rho u T}{\partial x} + c_p \frac{\partial \rho v T}{\partial y} = k_{eff} \frac{\partial^2 T}{\partial x^2} + k_{eff} \frac{\partial^2 T}{\partial y^2} + \frac{\partial p}{\partial t} + u \frac{\partial p}{\partial x} + v \frac{\partial p}{\partial y} \quad (9)$$

$$k_{eff} = \phi k + (1-\phi) k_s \quad (10)$$

Thermal gradients in the system develop due to the difference between indoor and outdoor conditions giving rise to natural convection. As mentioned previously, it is important to represent the effects of buoyancy on the flow to properly determine infiltration rates and the heat flux at the wall, so buoyancy is included in these simulations. A simple, temperature-dependent empirical equation of state for the fluid density, coupled with the body force term in the fluid y-momentum equation introduces the effects of buoyancy into the flow.

Results and Discussion

Simulations are performed for the five wall geometries under wind-induced pressures ranging from 0.1-10 Pa with a constant temperature difference of 24K between inside and

outside. Due to the complexity of the flow, it was not possible to achieve a converged solution using the steady-state equations. Therefore, the time-dependent equations were integrated in time until steady-state was reached. Comparison of results from simulations using a coarse computational grid (33,000 nodes) and a fine grid (140,000 nodes) for two different wall geometries show that the coarse grid is sufficient to provide a grid-independent solution. All results presented here are steady-state solutions from simulations using a 33,000 node grid.

The main point of interest is the extra energy load introduced by infiltration. This is determined by first calculating the heat flux through the room walls with no air leakage, designated as Q_o . Then, the energy flux is determined for the same wall types with air leakage. The difference between the two values is the infiltration-induced energy load. The convection and conduction energy fluxes across the external (outside) face of each wall are calculated for infiltrating and exfiltrating configurations. Using the external building face as the system control volume boundary is an arbitrary choice, the interior face could be used as well. However, it is important from an organizational standpoint that the energy accounting be performed at a consistent location.

For a given wall geometry, the infiltration air flow rate and energy flux vary with environmental conditions. The infiltration rate versus wind-induced pressure is shown in figure 3. In all cases, infiltration increases with wind pressure, but the actual values vary between geometries due to different flow resistances. The walls containing insulation (geometries 1-3) show a linear relationship between pressure and flow rate at pressures above about 0.5 Pa. This is the expected behavior, because the primary flow resistance in these cases, the insulation, is represented by linear flow-pressure relation, Darcy's Law. The empty walls (4-5) show a power law relationship with a pressure exponent of about 0.5 at pressures above about 0.5 Pa. The literature (1,8,11) shows that for typical residential dwellings pressure exponents range between one half to three quarters with averages typically about two-thirds. Although exponents up to unity are possible, they rarely play a significant role in adventitious leakage.

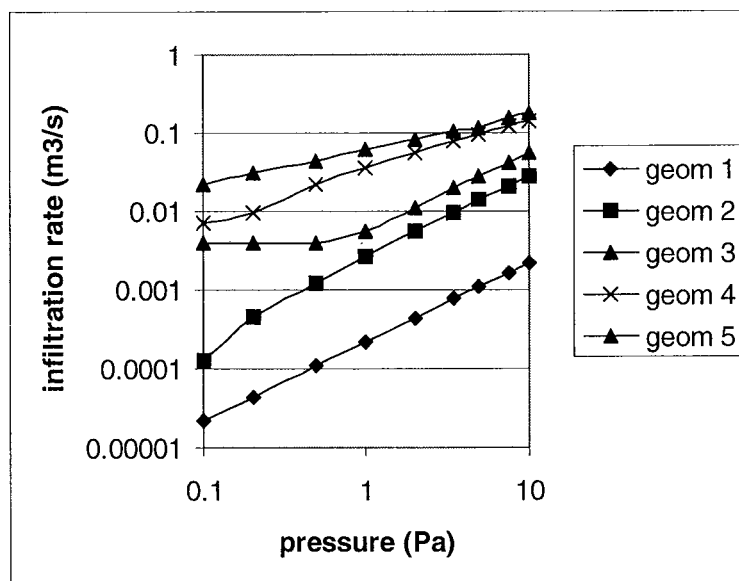


Figure 3: Infiltration rate vs. wind-induced pressure ($\Delta T=24K$, crack length=10 m).

Below 0.5 Pa, the influence of stack-induced pressure, due to thermal differences in the air, is comparable to that of the wind-induced pressure. It is interesting to note that with geometry 3, there is a low pressure plateau due to the stack effect and leak geometry.

The extra energy load due to infiltration, Q_{inf} , is represented as a fraction of the classical load, given by equation 1. The extra load, calculated via equation 11, uses the infiltration heat exchange effectiveness, ε , also known as the heat recovery factor, a non-dimensional factor introduced by Claridge (2,6,7), given in equation 12.

$$Q_{inf} = (1 - \varepsilon)\dot{m}c_p(T_i - T_o) \quad (11)$$

$$\varepsilon = 1 - \frac{Q - Q_o}{\dot{m}c_p\Delta T} \quad (12)$$

Figure 4 shows ε for the five wall geometries at various wind-induced pressures. In all cases, the heat recovery decreases with increasing flow rate. This is true for a given wall geometry over the range of pressures or in a comparison of different wall geometries at a given pressure. The heat transfer becomes less efficient at high flow rates because there is less time for energy to be transported from the walls to the infiltrating air.

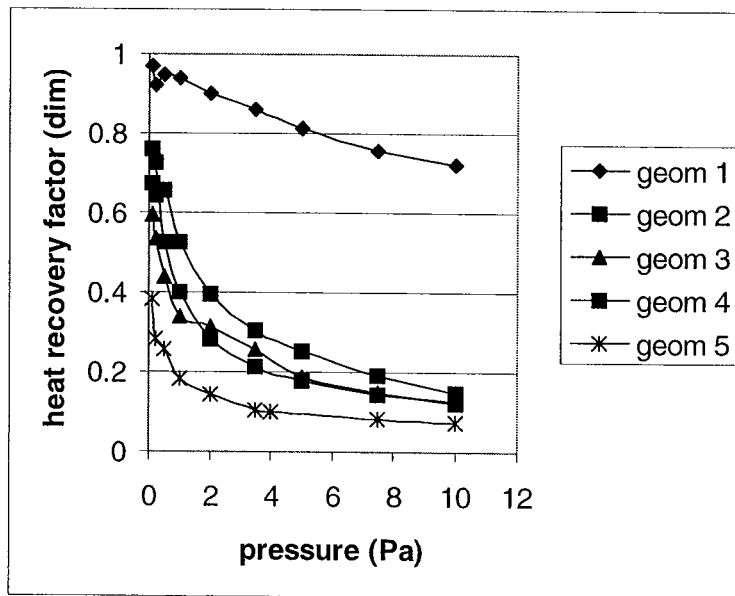


Figure 4: Heat recovery factor vs. wind-induced pressure for the five walls.

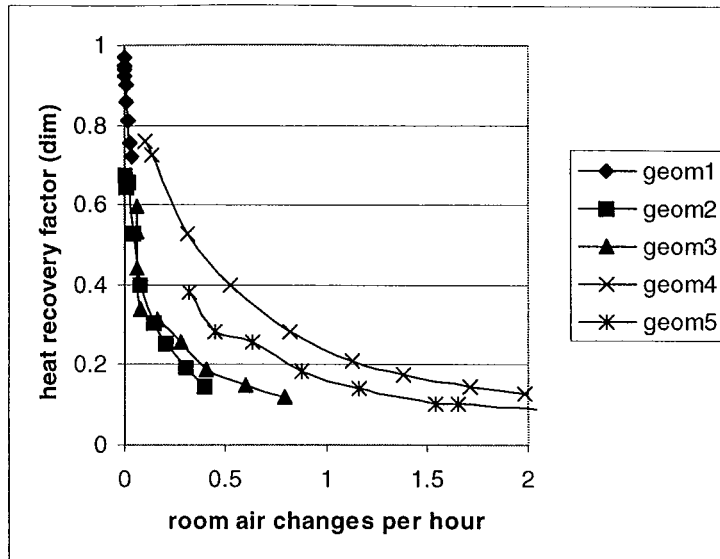


Figure 5: Heat recovery factor vs. infiltration rate in ACH.

Figure 5 shows that for a given infiltration rate (expressed here in room air changes per hour) and wall construction, insulated or empty, the heat recovery increases with infiltration path length. For example, wall geometries 4 and 5 are empty walls with long and short air flow paths, respectively. At a given infiltration rate the configuration with the long air flow path, geometry 4, has a higher heat recovery. Again, the increased heat recovery is due to longer transit times for infiltrating air in the wall. The same trend is true for geometries 1 and 2, but is more difficult to see on the graph. Another comparison can be made between walls with the same leakage configuration but different construction, insulated or empty. A comparison of geometries 2 and 5 at a given flow rate reveals that the empty wall, geometry 5, has a higher heat recovery, suggesting that wall construction, also, has an influence on heat recovery. This is because the thermal properties of the wall and the overall structure of the air flow in the wall cavity change with construction style.

An interesting point is revealed in comparison of geometries 2 and 3. Note that geometry 3 is similar to 2, except there are two holes instead of one. At pressures above about 0.5 Pa, geometry 3 has twice the flow as geometry 2, but nearly the same heat recovery. This indicates that in geometry 3 there is little interaction between the two holes, which is due to the large flow resistance of the insulation separating them. A wall of this design may not need to be modeled in its entirety. However, preliminary studies of this wall with an empty cavity show that there is a significant amount of interaction between the high and low holes, so this may not be a universal trait for all such wall designs. It is also interesting to note that the three insulated walls all seem to fall on a common curve, suggesting that a scaling law may apply. Future work on other configurations will be needed to explore these notions further.

In one sense, our results compare well with the experimental measurements of Claridge and Bhattacharyya (7). They calculated a maximum heat recovery of about 0.8 for a “diffuse” leakage path, which corresponds most closely to our geometry 1. This was nearly the average value determined in this study, as can be seen in figure 4.

In other ways, our results are not entirely comparable. In our simulations, we subjected each configuration to a range of pressures that are representative of the wind-induced pressures that real dwellings experience. For a given pressure, infiltration rates vary depending on the flow resistance (determined by the wall construction and environmental conditions), as can be seen in figures 3 and 5. In contrast, Claridge and Bhattacharyya adjusted the driving pressure to provide the same range of infiltration rates for each configuration. This technique is useful for some purposes, but the flow rates are too low to be representative of infiltration in most real dwellings, like our row-house scenario. When plotted against air change rate, all of their heat recovery values would be at very low air change rates, like our geometry 1 data. The infiltration rates for the configurations with “concentrated” leakage paths would be much higher (orders of magnitude) for realistic driving pressures.

Conclusions

Though still requiring substantiation, these results show the potential importance of infiltration heat recovery. The extent of heat recovery was found to be dependent on leakage path length, infiltration flow rate, and wall construction. In some circumstances, particularly in cases with low flow rates and long leakage paths, the heat recovery can be substantial, up to 95 percent. In these cases, the classical method will greatly over-predict the extra heating load due to infiltration. Even when the heat recovery is at the lowest level calculated, about 0.1, the classical method will over-predict the infiltration load by 10 percent. All leakage paths have not been represented in our simulations, but it seems that some modification should be considered to the classical method to increase its accuracy.

In reality, the importance of infiltration heat recovery will be determined by the particulars of the problem. For example, Sherman and Matson (14) found infiltration rates in typical U.S. housing stock to be around 1 ach. Our results suggest that about 10-20 percent of the heat would be recovered at these flow rates, so it seems unlikely that this mechanism plays a large role in the rather leaky envelopes of existing U.S. housing stock. In new construction, where infiltration rates can be quite low, infiltration heat recovery could be significant, provided the infiltrating air goes through the insulating layers and not just directly through holes. However, this leakage scenario is associated with high pressure exponents, which are not observed in most housing stock. Consequently, we would not expect this leakage scenario to occur, except in cases where it has been included in the design, as in dynamic insulation. So the infiltration heat recovery in most new houses would not be large.

The results in this report are limited to just a few test cases, but future work will include other wall geometries, more diverse environmental conditions, and integration of these findings into whole-building energy analysis models.

References

- 1) Baker, P. H., Sharples, S., Ward, I. C. (1987) “Air flow through cracks”, *Building and Environment*, Vol. 22, No. 4, pp. 293-304.
- 2) Bhattacharyya, S., Claridge, D. E. (1995) “The energy impact of air leakage through insulated walls”, *Transactions of the ASME*, Vol. 112, pp. 132-139.

- 3) Brunzell, J. T. (1995) "The indoor air quality and the ventilation performance of four occupied residential buildings with dynamic insulation", 16th AIVC Conference: Implementing the results of ventilation research, Palm Springs, USA, September 18-22, Proceedings Vol. 2, pp. 471-482.
- 4) Burns, P. J., Chow, L. C., Tien, C. L. (1977) "Convection in a vertical slot filled with porous insulation", *Int. J. Heat Mass Transfer*, Vol. 20, pp. 919-926.
- 5) Caffey, G. E. (1979) "Residential air infiltration", *ASHRAE Trans.*, Vol. 85, pp. 41-57.
- 6) Claridge, D. E., Liu, M. (1996) "The measured energy impact of infiltration in an outdoor test cell", *Transactions of the ASME*, Vol. 118, pp. 162-167.
- 7) Claridge, D. E., Bhattacharyya, S. (1990) "The measured impact of infiltration in a test cell", *J. Solar Energy Engineering*, Vol. 117, pp. 167-172.
- 8) Etheridge, D. W. (1988) "Modelling of air infiltration in single- and multi-cell buildings", *Energy and Buildings*, Vol. 10, pp. 185-192.
- 9) Jensen, L. (1993) "Energy impact of ventilation and dynamic insulation", 14th AIVC Conference: Energy impact of ventilation and air infiltration, Copenhagen, September 21-23, Proceedings, pp. 251-260.
- 10) Kohonen, R., Virtanen, M. (1987) "Thermal coupling of leakage flow and heating load of buildings", *ASHRAE Trans.*, Vol. 93, pp. 2303-2318.
- 11) Liddament, M. W. (1987) "Power law rules-- OK?", *Air Infiltration Review*, Vol. 8, No. 2, pp. 4-6.
- 12) "NIST estimates nationwide energy impact of air leakage in U. S. buildings" (1996) *J. Research of NIST*, Vol. 101, No. 3, p. 413.
- 13) Persily, A. (1982) "Understanding air infiltration in homes", Report PU/CEES No. 129, Princeton University Center for Energy and Environmental Studies, February, p. 335.
- 14) Sheman, M., Matson, N. (1993) "Ventilation-Energy liabilities in U.S. dwellings", 14th AIVC Conference: Energy impact of ventilation and air infiltration, Copenhagen, September 21-23, Proceedings, pp. 23-41.
- 15) Virtanen, M., Heimonen, I., Kohonen, R. (1992) "Application of the transfer function approach in the thermal analysis of dynamic wall structures", ASHRAE/DOE/BTECC Conference: Performance of the Exterior Envelopes of Buildings, December 7-10, Clearwater Beach, Florida, USA, Proceedings.



ERNEST ORLANDO LAWRENCE BERKELEY NATIONAL LABORATORY
ONE CYCLOTRON ROAD | BERKELEY, CALIFORNIA 94720